



Isolation of the Cyclosporin-Sensitive T Cell Transcription Factor NFATp

Patricia G. McCaffrey; Chun Luo; Tom K. Kerppola; Jugnu Jain; Tina M. Badalian;
Andrew M. Ho; Emmanuel Burgeon; William S. Lane; John N. Lambert; Tom Curran;
Gregory L. Verdine; Anjana Rao; Patrick G. Hogan

Science, New Series, Vol. 262, No. 5134. (Oct. 29, 1993), pp. 750-754.

Stable URL:

<http://links.jstor.org/sici?sici=0036-8075%2819931029%293%3A262%3A5134%3C750%3AIOTCTC%3E2.0.CO%3B2-R>

Science is currently published by American Association for the Advancement of Science.

Your use of the JSTOR archive indicates your acceptance of JSTOR's Terms and Conditions of Use, available at <http://www.jstor.org/about/terms.html>. JSTOR's Terms and Conditions of Use provides, in part, that unless you have obtained prior permission, you may not download an entire issue of a journal or multiple copies of articles, and you may use content in the JSTOR archive only for your personal, non-commercial use.

Please contact the publisher regarding any further use of this work. Publisher contact information may be obtained at <http://www.jstor.org/journals/aaas.html>.

Each copy of any part of a JSTOR transmission must contain the same copyright notice that appears on the screen or printed page of such transmission.

JSTOR is an independent not-for-profit organization dedicated to creating and preserving a digital archive of scholarly journals. For more information regarding JSTOR, please contact support@jstor.org.

12. M. Kozak, *J. Cell. Biol.* **108**, 229 (1989).
13. Sequences were analyzed with the Genetics Computer Group (GCG) programs on a mainframe computer. Sequence homology searches were carried out through the BLAST E-mail server at the National Center for Biotechnology Information, National Library of Medicine, Bethesda, MD.
14. T. El-Baradi and T. Pieler, *Mech. Dev.* **35**, 155 (1991).
15. J.-P. Kerckaert *et al.*, *Nat. Genet.* **5**, 66 (1993).
16. U. B. Rosenberg *et al.*, *Nature* **319**, 336 (1986); E. J. Bellefroid *et al.*, *DNA* **8**, 377 (1989).
17. W. Knochel *et al.*, *Proc. Natl. Acad. Sci. U.S.A.* **86**, 6097 (1989).
18. E. J. Bellefroid, D. A. Poncelet, P. J. Lecocq, O. Revelant, J. A. Martial, *ibid.* **88**, 3608 (1991).
19. M. M. Sugawara *et al.*, listed as unpublished sequence in NewGenBank (29 May 1993).
20. S. D. Harrison and A. A. Travers, *EMBO J.* **9**, 207 (1990); P. R. DiBello, D. A. Withers, C. A. Bayer, J. W. Fristrom, G. M. Guild, *Genetics* **129**, 385 (1991).
21. P. Chardin, G. Courtois, M.-G. Mattei, S. Gisselbrecht, *Nucleic Acid Res.* **19**, 1431 (1991).
22. Z. Chen *et al.*, *EMBO J.* **12**, 1161 (1993).
23. E. V. Koonin, T. G. Senkevich, V. I. Chermos, *Trends Biochem. Sci.* **17**, 213 (1992).
24. F. Xue and L. Cooley, *Cell* **72**, 681 (1993).
25. B. H. Ye *et al.*, unpublished data.
26. A phage genomic library constructed from normal human placenta DNA (Stratagene) was screened (8×10^5 plaques) with the *BCL-6* cDNA (11). Twelve overlapping clones spanning ~50 kb of genomic DNA were isolated. After restriction mapping, the position of various *BCL-6* exons was determined by Southern hybridization with various cDNA probes.
27. A *BCL-6* transcript of normal size was detected by Northern blot analysis of DLCL cells carrying either normal or truncated *BCL-6*. Some of the truncations were in the 5' flanking sequences and would therefore not be expected to generate structurally abnormal transcripts.
28. P.M.L., H. de Thé *et al.*, *Cell* **66**, 675 (1991); A. Kazizuka *et al.*, *ibid.*, p. 663; P. P. Pandolfi *et al.*, *Oncogene* **6**, 1285 (1991); *EVI-1*, K. Morishita *et al.*, *Cell* **54**, 831 (1988); S. Fichelson *et al.*, *Leukemia* **6**, 93 (1992); *TTG-1*, E. A. McGuire *et al.*, *Mol. Cell. Biol.* **9**, 2124 (1989); *HTRX*, M. Djabali *et al.*, *Nat. Genet.* **2**, 113 (1992); D. C. Tkachuk, S. Kohler, M. L. Cleary, *Cell* **71**, 691 (1992); Y. Gu *et al.*, *ibid.*, p. 701; *WT-1*, D. A. Haber *et al.*, *ibid.* **61**, 1257 (1990).
29. L. J. Medeiros *et al.*, in (2), pp. 263–298.
30. Abbreviations for the amino acid residues are A, Ala; C, Cys; D, Asp; E, Glu; F, Phe; G, Gly; H, His; I, Ile; K, Lys; L, Leu; M, Met; N, Asn; P, Pro; Q, Gln; R, Arg; S, Ser; T, Thr; V, Val; W, Trp; and Y, Tyr.
31. We thank Y. Zhang, S. Shammah, C.-C. Chang, G. Gaidano, and T. Saksela for reagents and advice. Supported by NIH grants CA 44029 (R.D.-F.), CA 48236 and EY 06337 (D.M.K.), and CA 34775 and CA 08748 (R.S.K.C.). F.L.C. is supported in part by Associazione Italiana contro le Leucemie (AIL).

9 July 1993; accepted 31 August 1993

Isolation of the Cyclosporin-Sensitive T Cell Transcription Factor NFATp

Patricia G. McCaffrey, Chun Luo, Tom K. Kerppola, Jugnu Jain, Tina M. Badalian, Andrew M. Ho, Emmanuel Burgeon, William S. Lane, John N. Lambert, Tom Curran, Gregory L. Verdine, Anjana Rao,* Patrick G. Hogan

Nuclear factor of activated T cells (NFAT) is a transcription factor that regulates expression of the cytokine interleukin-2 (IL-2) in activated T cells. The DNA-binding specificity of NFAT is conferred by NFATp, a phosphoprotein that is a target for the immunosuppressive compounds cyclosporin A and FK506. Here, the purification of NFATp from murine T cells and the isolation of a complementary DNA clone encoding NFATp are reported. A truncated form of NFATp, expressed as a recombinant protein in bacteria, binds specifically to the NFAT site of the murine IL-2 promoter and forms a transcriptionally active complex with recombinant c-Fos and c-Jun. Antisera to tryptic peptides of the purified protein or to the recombinant protein fragment react with T cell NFATp. The molecular cloning of NFATp should allow detailed analysis of a T cell transcription factor that is central to initiation of the immune response.

Nuclear factor of activated T cells is an inducible DNA-binding protein that binds to two independent sites in the IL-2 promoter (1, 2). NFAT is a multisubunit transcription factor (3) consisting of at least three DNA-binding polypeptides, the pre-existing subunit NFATp (4–6) and homodimers or heterodimers of Fos and Jun family proteins (6–9). NFATp is present in

the cytosolic fraction of unstimulated T cells (3–7); after T cell activation, it is found in nuclear extracts and forms DNA-protein complexes with Fos and Jun family members at the NFAT sites of the IL-2 promoter (3, 5–9). NFATp has also been implicated in the transcriptional regulation of other cytokine genes, including the genes for granulocyte-macrophage colony-stimulating factor (GM-CSF), IL-3, IL-4, and tumor necrosis factor- α (TNF- α) (10).

NFATp is the target of a Ca^{2+} -dependent signaling pathway initiated at the T cell receptor (3, 4, 6, 7, 11–13). The rise in intracellular free Ca^{2+} in activated T cells results in an increase in the phosphatase activity of the Ca^{2+} - and calmodulin-dependent phosphatase calcineurin (14). NFATp is a substrate for calcineurin in vitro (4, 6) and is thought to be dephosphorylated by calcineurin in activated T cells, resulting in its translocation from the cytoplasm to the nucleus (13). Cyclosporin

A (CsA) and FK506, which act as a complex with their respective intracellular receptors to inhibit the phosphatase activity of calcineurin (15), block the dephosphorylation of NFATp (4) and the appearance of NFAT in nuclear extracts of stimulated T cells (2, 3, 7, 12). This mechanism may account for the sensitivity to cyclosporin of IL-2 and other cytokine genes (10, 13) and thus for the profound immunosuppression caused by CsA and FK506 (13).

NFATp was purified from the C1.7W2 cell line (16), a derivative of the murine T cell clone Ar-5 (17), by ammonium sulfate fractionation followed by successive chromatography on a heparin-agarose column and an NFAT oligonucleotide affinity column (18). A silver-stained SDS gel of the purified protein showed a major broad band migrating with an apparent molecular size of ~120 kD (Fig. 1, top). We have shown that this band contains a DNA-binding phosphoprotein that is dephosphorylated by calcineurin to yield four sharp bands migrating with apparent molecular sizes of ~110 to 115 kD (6). NFATp DNA-binding activity was demonstrable in protein eluted from the SDS gel and renatured (4), and more than 90% of the activity recovered from the gel comigrated with the ~120-kD band (Fig. 1, lane 7). The faster migrating complexes formed with proteins of slightly smaller molecular size (lanes 8 to 11) most likely derive from partial proteolysis. The purified protein binds to the NFAT site with the appropriate specificity and forms a DNA-protein complex with recombinant Fos and Jun (6).

To confirm that the 120-kD protein was the preexisting subunit of the T cell transcription factor NFAT, we used antisera to tryptic peptides derived from the 120-kD protein (18). When one such antiserum (to peptide 72) was included in the binding reaction, it "supershifted" the NFATp-DNA complex formed by the cytosolic fraction from unstimulated T cells (Fig. 2, lane

P. G. McCaffrey, C. Luo, J. Jain, T. M. Badalian, E. Burgeon, A. Rao, Division of Tumor Virology, Dana-Farber Cancer Institute, and Department of Pathology, Harvard Medical School, Boston, MA 02115.

T. K. Kerppola and T. Curran, Department of Molecular Oncology and Virology, Roche Institute of Molecular Biology, Roche Research Center, Nutley, NJ 07110.

A. M. Ho and P. G. Hogan, Department of Neurobiology, Harvard Medical School, Boston, MA 02115.

W. S. Lane, Microchemistry Facility, Harvard University, Cambridge, MA 02138.

J. N. Lambert and G. L. Verdine, Department of Chemistry, Harvard University, Cambridge, MA 02138.

*To whom correspondence should be addressed.

3), as well as both NFAT complexes formed by nuclear extracts from stimulated T cells (lane 8). The effect of the serum was prevented by preincubation with its cognate peptide (lanes 4 and 9), but not by

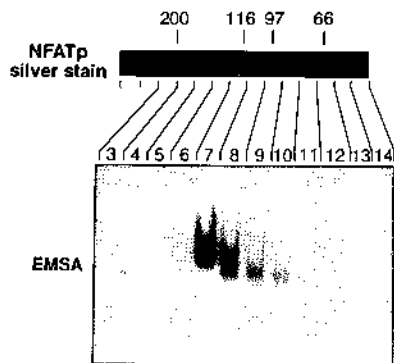


Fig. 1. Analysis of purified NFATp by renaturation of NFATp activity after SDS-PAGE. (Top) Purified NFATp (50 ng) was subjected to electrophoresis on an analytical 6% SDS-polyacrylamide gel and subsequently silver-stained (Pierce Gel-code kit). (Bottom) A second lane of the same gel was loaded with 50 ng of the purified protein. After electrophoresis, the gel was sliced, proteins were eluted from gel slices and renatured, and the fractionated proteins were evaluated in an electrophoretic mobility-shift assay for the ability to bind to the NFAT site of the murine IL-2 promoter (4).

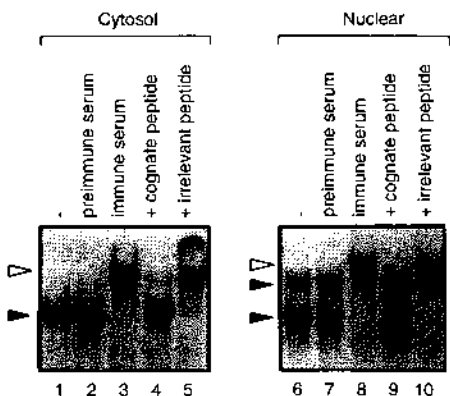


Fig. 2. Antisera to tryptic peptides of purified NFATp react with NFATp in T cell extracts. Cytosolic extracts (4) from unstimulated Ar-5 T cells (lanes 1 to 5) or nuclear extracts (23) from Ar-5 T cells stimulated with antibody to CD3 (anti-CD3) (lanes 6 to 10) were incubated without antiserum (lanes 1 and 6), with antiserum to peptide 72 (immune, lanes 3 and 8), or with serum from the same rabbit taken before immunization (preimmune, lanes 2 and 7), then analyzed by gel-shift assay for binding to the NFAT oligonucleotide (7). For peptide competition, 1 μ g of peptide 72 (lanes 4 and 9) or peptide 25 (lanes 5 and 10) was mixed with the antiserum before it was added to cell extracts. Filled arrowheads identify the cytosolic NFATp, nuclear NFATp, and nuclear NFATp-Fos-Jun complexes; open arrowheads indicate the "supershifted" complexes; the unmarked complex results from binding of serum proteins.

preincubation with a different peptide (lanes 5 and 10). Preimmune serum had no effect on binding (lanes 2 and 7). Similar effects were seen with antisera to peptides 23.1 and 25. These data demonstrate that the purified protein is NFATp.

In order to isolate a cDNA clone for NFATp, we used degenerate oligonucleotides based on the sequences of two tryptic peptides of purified NFATp in a polymerase chain reaction (PCR) to amplify an ~800-bp fragment from C1.7W2 cDNA, and the fragment was used to screen a cDNA library from murine T cells (19). The longest clone isolated contains an insert of ~4.5 kb in length, with an open reading frame extending 2672 base pairs (bp) from the 5' end of the insert and with ~1.8 kb of 3' untranslated region that does not extend to the polyadenylate tail. The open reading frame encodes a polypeptide of 890 amino acids

```

1  GSSASPTISDTFSFYTSFCVSNWAGPDDLCPCQFNIPARVSPRTSPFMS
51  RTSLAEDSCLGRHSFVFRPASRSSSPGAKRRSCAEALVAFLEPAASQPS
101  RSPSPQSPPEVAPQDSDIFAGYPPTAGSAVLMALNTLATDSPCGIIPSKI
151  WKTSPOPTFVSTAPSKAGLARIHYPTVFLGFCQEQERRNSAPESILLVP
201  PTVPRQLVPAIPIKCSIPTVATSLFPEWPLSNQSGSYELREIVQSPHEDRA
251  RYETEGSRGAVRAPYQGGFPVQLEGYMNKPLGLQIFIGTADERILKPHA
301  FYQVVRITGKTVTTTYSYKIVGNTRVLEIPLPKRWRATIDCAGTILKLR
351  NADIELRKGEDIDIGRNTVRLVFRVVEVPEPSGRIVSLQAASNPIECSQR
401  SAHELPMVERQDMDSCLVYGGQQMLTGQNFPTAESKVVMEKTTDGGQIVH
451  EHEATVQKDRSQPNMLFVEIPEYRNKHIREVPPVKNFYVINGRKRKRSQPQH
501  FTYKVPVPAINTPEPSDEYEPLSGLCSPAHGGLGSQVYVQHPMLAESPSCLV
551  ATKAPCCQFRGLGSSPDARYQQSSPAALYGRSSKLSLPGLLGYQQPSLLA
601  APDGLADARSRVLRVHAGSQGGQGGSTLEHTSSASQASPVVYHSPTWQQL
651  RGGGNGEFQHEIMVCFNFGPSARMPPPPINQGRLLSPGAYPTVYQQQTAP
701  SQRAAINGPSPDQKEALPGVTVKQEQNLQTYLDDAATSSEWVGTERYIE
751  RRFWRKTLVQPGILLPSFLLGLSLAGPSSQTPSERKPIEEDVFLSCSQIA
801  WCCQRFPLSTCFVLPGLAVEWEGQLGRGLEPIPWAPDSAGSLHEVDSVG
851  LAGVYGVNLLYLHNFSDQGNQTFSPHWQRKREVASPCGW
    
```

Fig. 3. Deduced amino acid sequence of NFATp. The underlined sequences match the sequences of tryptic peptides from purified NFATp. X in the underlining for peptides 23.3 and 72 indicates positions at which the identity of the amino acid could not be determined unambiguously. The arrowheads delimit the NFATp sequence contained within the recombinant protein that was expressed in bacteria. The sequence of murine NFATp has been deposited with GenBank (accession number U02079). Single-letter abbreviations for the amino acid residues are as follows: A, Ala; C, Cys; D, Asp; E, Glu; F, Phe; G, Gly; H, His; I, Ile; K, Lys; L, Leu; M, Met; N, Asn; P, Pro; Q, Gln; R, Arg; S, Ser; T, Thr; V, Val; W, Trp; and Y, Tyr.

(Fig. 3) that contains eight of nine tryptic peptides identified by sequencing of purified NFATp. The cDNA insert may lack a small amount of coding sequence at the 5' end, because the predicted molecular size of the encoded protein (97 kD) is somewhat smaller than the apparent molecular size of dephosphorylated NFATp [110 to 115 kD (6)] and because one tryptic peptide from purified NFATp is unaccounted for in the encoded protein. A search of the Genbank DNA and protein databases with the Blast algorithm (20) indicated that the cDNA encodes a previously unidentified protein. A 464-amino acid fragment containing the DNA-binding domain displayed a limited similarity to the rel homology domain of human and murine RelA (p65) (18.9 and 17.8% amino acid identity, respectively, over 428 amino acids). A preliminary analysis of additional cDNA clones indicates that T cells express at least three forms of NFATp related to each other by alternative splicing and differing at their COOH-termini.

The T cell lines C1.7W2 and Ar-5, but not L cells, express NFATp mRNA (Fig. 4), consistent with our previous demonstration that NFATp protein is present in T cells but not in L cells (4). The ~800-bp PCR fragment hybridized to a transcript of ~8–9 kb expressed in the C1.7W2 T cell line used for purification of NFATp (lane 1) and in the untransformed T cell clone Ar-5 used to generate the cDNA library (lane 2), but did not hybridize to any transcript expressed in L cells (lane 3). Two other cDNA probes representing different parts of the coding region of NFATp gave similar results. We are presently undertaking a

Fig. 4. Northern (RNA) analysis of NFATp mRNA in T cell and fibroblast cell lines. Cytoplasmic RNA from the murine T cell clone Ar-5, the transformed T cell line C1.7W2, and the murine fibroblast L cell line were separated by electrophoresis in formaldehyde gels, transferred to nylon, and hybridized with a labeled fragment of NFATp coding sequence corresponding to the ~800-bp PCR product. The positions of the major NFATp transcript (arrow) and of the 28S and 18S ribosomal RNAs are indicated. The lower panel shows ethidium bromide staining of the RNA before transfer to nitrocellulose indicating that the RNA was intact and that equivalent amounts of RNA were loaded in each lane.

systematic analysis of the tissue distribution of NFATp by protein immunoblotting analysis and quantitative PCR.

To test directly whether the cDNA encoded a protein with the characteristics of NFATp, we examined the ability of a recombinant fragment of the protein to bind to the NFAT site of the murine IL-2 promoter and to associate with Fos and Jun. A 464-amino acid fragment of the protein (sequence between arrowheads in Fig. 3) was expressed as a hexahistidine-tagged protein in bacteria (21). This recombinant protein bound to the NFAT oligonucleotide in a gel-shift assay (Fig. 5A, lane 1). Its binding specificity was identical to that of authentic T cell NFATp (4-7), as judged by competition with excess unlabeled NFAT oligonucleotide (lane 2) and the mutant NFAT oligonucleotides M1 to M3 (lanes 3 to 5). The M1 oligonucleotide (lane 3) is mutated in four bases remote from the NFAT binding site and competes as strongly for binding as the authentic NFAT oligonucleotide; the M2 oligonucleotide (lane 4) is mutated in four bases located between the M1 and M3 regions and competes with intermediate efficiency; and the M3 oligonucleotide (lane 5) is mutated in the GGAA tetranucleotide sequence essential for binding of NFATp (4-7, 22, 23) and does not compete for binding. Methylation interference analysis also showed that binding of the recombinant protein to the NFAT site required the GGAA core binding region, as previously demonstrated for NFAT (22, 23). Like NFATp purified from T cells (6), the recombinant protein associated with homodimers of c-Jun or with heterodimers of c-Fos and c-Jun, but not with c-Fos alone, to form a DNA-protein complex that migrated with slower mobility than the NFATp-DNA complex in a gel-shift assay (lanes 7 to 9). The c-Fos and c-Jun proteins do not bind to the NFAT oligonucleotide in the absence of NFATp (lane 10). The complex containing c-Fos and c-Jun resembled the nuclear complex of NFATp, Fos, and Jun in that its formation was competed by excess unlabeled activator protein 1 (AP-1) oligonucleotide. These data indicate that a ~50-kD fragment of NFATp is sufficient to account for the DNA-binding properties of NFATp and for its ability to associate with Fos and Jun proteins.

Evidence that the cDNA clone encodes NFATp was provided by the ability of antisera to the recombinant protein to react specifically with NFATp from cytosolic or nuclear extracts of T cells. When serum from a rabbit immunized with the recombinant protein (21) was included in the gel-shift assay, a small proportion of the NFATp-DNA complexes were "super-shifted" (Fig. 6, lane 3), and most of the

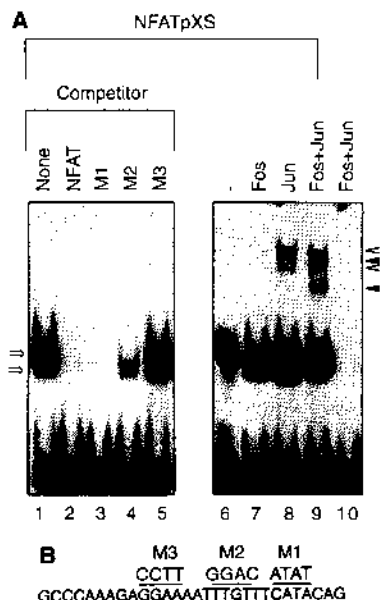


Fig. 5. Binding of a recombinant fragment of NFATp (NFATpXS) to DNA and association with Fos and Jun proteins. **(A)** Lanes 1 to 5, binding of the recombinant fragment of NFATp (21) to the distal NFAT site of the murine IL-2 promoter was assessed by electrophoretic mobility-shift assay (4) in the presence or absence of a 200-fold excess of unlabeled competitor oligonucleotides. The arrows indicate two DNA-protein complexes formed with NFATpXS. Lanes 7 to 9, full-length recombinant c-Fos and c-Jun proteins (30) were included in the binding reactions. The open arrows indicate Jun-Jun-NFATpXS complexes, whereas the closed arrows indicate Fos-Jun-NFATpXS complexes. Lane 10, Fos and Jun proteins do not bind to the NFAT oligonucleotide. **(B)** Sequences of competitor oligonucleotides.

DNA-protein complexes appeared to be in large aggregates (lanes 3 and 7). The predominance of large aggregates probably reflects recognition by the serum of multiple antigenic determinants on NFATp. Preimmune serum from the same rabbit did not alter the mobility of NFATp-DNA and NFATp-DNA complexes (lanes 2 and 6).

To examine the role of the cloned NFATp protein in transcription, we tested the effect of the recombinant NFATp fragment on transcription *in vitro* from a template containing three NFAT sites upstream of the murine IL-2 promoter (Fig. 7). The same plasmid has been used to demonstrate transcriptional activation *in vivo* in response to stimulation with antigen (7). A combination of the recombinant NFATp fragment with c-Fos and c-Jun, or with c-Jun only, activated transcription from this construct (Fig. 7, lanes 2 and 3). In combination with NFATp, a Jun deletion derivative (J91-334) lacking the NH₂-terminal repressor domain was a more potent activator than full-length Jun (lanes 6, 7, and 14), as previously observed for tran-

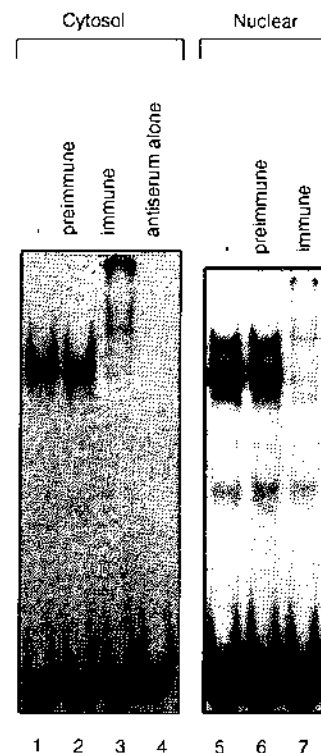
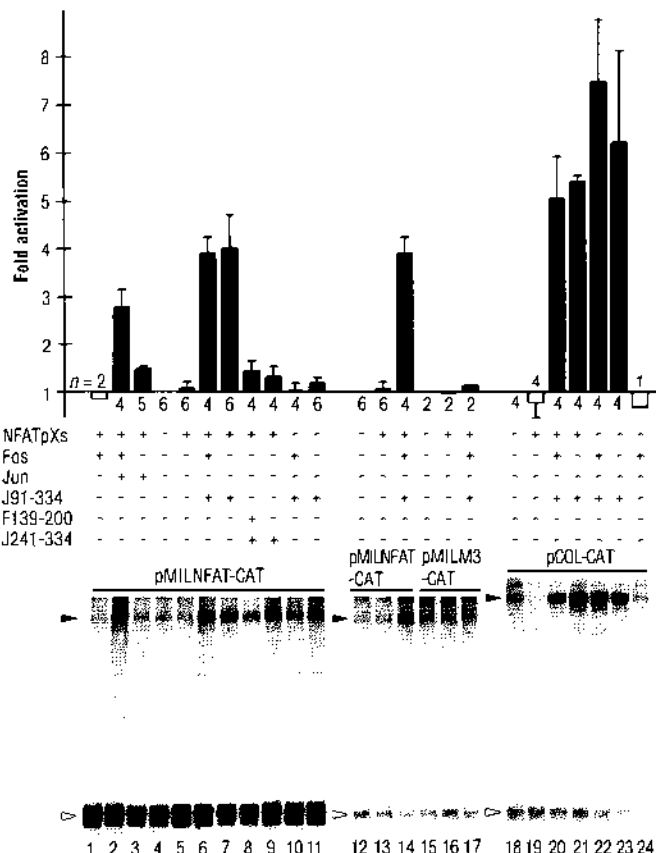


Fig. 6. Antisera to recombinant NFATp react with NFATp in T cell extracts. Cytosolic extracts from unstimulated Ar-5 T cells or nuclear extracts from cells stimulated with anti-CD3 were incubated without antiserum (lanes 1 and 5), with an antiserum to the recombinant NFATp fragment (21) (lanes 3 and 7), or with preimmune serum from the same rabbit (lanes 2 and 6), followed by gel-shift analysis of binding to the NFAT oligonucleotide.

scriptional activation by Jun at AP-1 sites (24). In contrast, neither the truncated NFATp alone nor AP-1 proteins alone had a notable effect (lanes 5, 10, and 11). Truncated Fos and Jun proteins (F139-200 and J241-334) containing the dimerization and DNA-binding domains but lacking transcriptional activation domains are able to form a complex with NFATp (6). However, they did not activate transcription in conjunction with truncated NFATp (lanes 8 and 9), indicating that the truncated NFATp is not transcriptionally active in the absence of Fos and Jun. No notable transcriptional activation was observed when a template containing a mutated NFAT site incapable of binding NFATp was used (lanes 15 to 17). Moreover, the truncated NFATp had no effect on transcription activated by Fos and Jun on a template containing an AP-1 site (lanes 18 to 24), consistent with our previous observation that NFATp does not form a complex with Fos and Jun on the AP-1 site (6).

These data show that truncated NFATp forms a transcriptionally active complex with Fos and Jun at the IL-2 promoter

Fig. 7. Transcriptional activation by NFATp, c-Fos, and c-Jun on different templates. The templates indicated above the lanes were incubated with the proteins listed and transcribed in vitro in Narnawa nuclear extracts (24, 31). The pMILNFAT-CAT construct (lanes 1 to 14) contains three NFAT sites upstream of the basal IL-2 promoter (7). The pMILM3-CAT construct (lanes 15 to 17) contains four NFAT sites in which critical contact residues have been altered (7). The pCOL-CAT construct (lanes 18 to 24) contains three NFAT sites upstream of the basal IL-2 promoter (7). The pMILNFAT-CAT construct (lanes 1 to 14) contains three NFAT sites upstream of the basal IL-2 promoter (7). The pMILM3-CAT construct (lanes 15 to 17) contains four NFAT sites in which critical contact residues have been altered (7). The pCOL-CAT construct (lanes 18 to 24) contains three NFAT sites upstream of the basal IL-2 promoter (7). Transcripts were resolved on denaturing polyacrylamide gels and quantitated with the use of a phosphorimager. The filled arrowheads point to the specific transcripts and the open arrowheads to internal controls. Transcription in the presence of different combinations of proteins was expressed relative to a reaction in the absence of recombinant proteins (fold activation). The average of several independent experiments (number shown at the base of each bar) and the standard deviation in cases where more than three independent experiments were performed are shown (solid bars, activation; open bars, repression).



NFAT site. They are consistent with the interpretation that NFATp primarily determines the DNA-binding specificity of the NFAT complex in vivo, whereas at least a portion of the transcriptional activity is provided by Fos and Jun. Because the current experiments were performed with a truncated NFATp, they do not exclude the possibility that full-length NFATp has a transcriptional activation domain that can function in the absence of Fos and Jun. However, there is evidence suggesting that Fos and Jun family proteins are required along with NFATp to activate transcription at the IL-2 promoter NFAT site in vivo, since mutations in the NFAT site that prevent the association of Fos and Jun with NFATp abolish the function of this site in activated T cells (8).

The cDNA clone reported here fulfills four essential criteria defining NFATp: (i) the mRNA is expressed in T cells but not in fibroblasts, (ii) a recombinant fragment of the protein binds specifically to the NFAT site, (iii) the recombinant protein fragment forms a transcriptionally active complex with Fos and Jun on the NFAT DNA sequence, and (iv) antibodies to the recombinant protein specifically react with

NFATp in T cell extracts. The recombinant protein defines a functional 464-amino acid fragment of NFATp that contains the domains required for DNA binding and for formation of a transcriptionally active complex with Fos and Jun. The cloning of this previously uncharacterized DNA-binding protein makes possible detailed studies of its structure, its interactions with other transcription factors and with specific sites in DNA, its role in the induction of IL-2 and other cytokine genes, and its regulation by calcineurin during T cell activation.

REFERENCES AND NOTES

1. J. P. Shaw *et al.*, *Science* **241**, 202 (1988).
2. T. Brabletz, I. Pietrowski, E. Serfling, *Nucleic Acids Res.* **19**, 61 (1991).
3. W. M. Flanagan, B. Corthésy, R. J. Bram, G. R. Crabtree, *Nature* **352**, 803 (1991).
4. P. G. McCaffrey, B. A. Perrino, T. R. Soderling, A. Rao, *J. Biol. Chem.* **268**, 3747 (1993).
5. J. Jain, P. G. McCaffrey, V. E. Valge-Archer, A. Rao, *Nature* **356**, 801 (1992).
6. J. Jain *et al.*, *ibid.* **365**, 352 (1993).
7. J. Jain, Z. Miner, A. Rao, *J. Immunol.* **151**, 837 (1993).
8. L. H. Boise *et al.*, *Mol. Cell. Biol.* **13**, 1911 (1993).
9. J. P. Northrop, K. S. Ullman, G. R. Crabtree, *J. Biol. Chem.* **268**, 2917 (1993).
10. P. N. Cockerill, M. F. Shannon, A. G. Bert, G. R. Ryan, M. A. Vadas, *Proc. Natl. Acad. Sci. U.S.A.*

- 90, 2466 (1993); S. J. Szabo, J. S. Gold, T. L. Murphy, K. M. Murphy, *Mol. Cell. Biol.* **13**, 4793 (1993); A. E. Goldfeld, P. G. McCaffrey, J. L. Strominger, A. Rao, *J. Exp. Med.* **178**, 1365 (1993); J. W. Rooney, M. R. Hodge, P. G. McCaffrey, A. Rao, L. H. Glimcher, in preparation.
11. N. A. Clipstone and G. R. Crabtree, *Nature* **357**, 695 (1992).
12. P. S. Mattila *et al.*, *EMBO J.* **9**, 4425 (1990).
13. S. L. Schreiber and G. R. Crabtree, *Immunol. Today* **13**, 136 (1992); J. Liu, *ibid.* **14**, 290 (1993).
14. D. A. Fruman, C. B. Klee, B. E. Bierer, S. J. Burakoff, *Proc. Natl. Acad. Sci. U.S.A.* **89**, 3686 (1992).
15. J. Liu *et al.*, *Cell* **66**, 807 (1991).
16. V. E. Valge-Archer, J. de Villiers, A. J. Sinskey, A. Rao, *J. Immunol.* **145**, 4355 (1990).
17. A. Rao, S. J. Faas, H. Cantor, *J. Exp. Med.* **159**, 479 (1984).
18. CI.7W2 cell extracts were prepared by NP-40 lysis and ammonium sulfate precipitation as described (4). The precipitated protein (1.2 g from 10¹¹ cells) was dialyzed against buffer A [150 mM NaCl, 20 mM Hepes (pH 7.4), 2 mM EDTA, 0.5 mM dithiothreitol, 10% glycerol], supplemented with protease inhibitors [aprotinin (100 µg/ml), 2.5 µM leupeptin, and 2 mM phenylmethylsulfonyl fluoride] and loaded onto a 30-ml heparin-agarose column (Sigma). The column was washed with 10 column volumes of the same buffer containing 200 mM NaCl, and bound protein was eluted with a linear gradient of 0.2 to 1.0 M NaCl in a total volume of 250 ml. The NFATp activity was determined by electrophoretic mobility-shift assay as described (4, 7). Active fractions were combined and dialyzed overnight against buffer A. The dialyzed pool (90 ml, 95 mg of protein) was loaded in 20-mg batches onto a 1-ml high-capacity oligonucleotide affinity column (25) in the presence of sheared herring sperm DNA (200 µg/ml). The column was washed with the same buffer, and NFAT was eluted with a linear gradient of 0.15 to 1.0 M NaCl. The NFAT activity eluted in fractions between 0.4 and 0.6 M NaCl. The peak fractions from several separate fractionations were combined, dialyzed against buffer containing 150 mM NaCl, and reloaded onto the same affinity column. After two cycles over the affinity column, ~10 µg of highly purified NFATp was obtained. This material bound specifically to the NFAT site, was a phosphoprotein substrate for calcineurin, and associated with c-Fos and c-Jun to form the NFAT-Fos-Jun ternary complex on the NFAT site oligonucleotide (6). Renaturation from gel slices and electrophoretic mobility-shift assays were done as described (4). The purified NFATp protein was acetone precipitated, subjected to electrophoresis on a 6% SDS-polyacrylamide gel, and transferred to nitrocellulose. The NFATp band was localized by Ponceau Red staining, excised, and digested with trypsin in situ. The resultant peptides were separated by microbore high-performance liquid chromatography, analyzed by laser desorption mass spectrometry, and Edman microsequenced. Strategies for the selection of peptide fractions and their microsequencing have been described (26). For generation of antisera to peptide 72, rabbits were immunized with a 21-amino acid synthetic peptide conjugated to keyhole limpet hemocyanin (27).
19. Degenerate oligonucleotides based on the sequences of peptides 23.2 and 25 were used in a PCR to amplify an ~800-bp fragment from CI.7W2 cDNA. The fragment was used to screen an amplified cDNA library (representing 10⁶ primary plaques) in λ ZAPII (Stratagene), generated by oligo(dT) and random priming of cytoplasmic polyadenylated mRNA from Ar-5 T cells. After plaque purification of the recombinant λ bacteriophage clones and excision of pBluescript phagemids carrying the cDNA inserts, the coding sequences of several cDNA clones were determined by sequencing of both strands using the dideoxy chain termination method (28).
20. S. F. Altschul, W. Gish, W. Miller, E. W. Myers, D.

- J. Lipman, *J. Mol. Biol.* 215, 403 (1990).
21. A cDNA fragment common to all the alternatively spliced cDNAs was excised by digestion with Xho I and Sma I, subcloned into the vector pQE-31 (Qiagen), and expressed as a hexahistidine-tagged protein in bacteria (29). The expressed protein contained an additional 18 vector-encoded amino acids (MRGSHHHHHHTAPHASSV) at the NH₂-terminus and 9 amino acids (VDLEPSLIS) at the COOH-terminus of the sequence indicated between the arrowheads in Fig. 3. The recombinant protein was purified by chromatography on a nickel-chelate column in 8 M urea, and elution was with 250 mM imidazole. After dialysis against buffer A (18), the protein was assayed for DNA binding and association with Fos and Jun as described for NFATp purified from T cells (6). To generate antisera, we immunized rabbits with the purified recombinant NFATp.
 22. C. Randak, T. Brabletz, M. Hergenrother, I. Sobotta, E. Serfling, *EMBO J.* 9, 2529 (1990); C. B. Thompson *et al.*, *Mol. Cell. Biol.* 12, 1043 (1992).
 23. P. G. McCaffrey, J. Jain, C. Jamieson, R. Sen, A. Rao, *J. Biol. Chem.* 267, 1864 (1992).
 24. T. K. Kerppola, D. Luk, T. Curran, *Mol. Cell. Biol.* 13, 3782 (1993).
 25. C. J. Larson and G. L. Verdine, *Nucleic Acids Res.* 20, 3525 (1992).
 26. W. S. Lane, A. Galat, M. W. Harding, S. L. Schreiber, *J. Protein Chem.* 10, 151 (1991).
 27. G. Walter, K.-H. Scheidtmann, A. Carbone, A. P. Laudano, R. F. Doolittle, *Proc. Natl. Acad. Sci. U.S.A.* 77, 5197 (1980).
 28. F. Sanger, S. Nicklen, A. R. Coulson, *ibid.* 74, 5463 (1977).
 29. C. Abate, D. Luk, R. Gentz, F. J. Rauscher, T. Curran, *ibid.* 87, 1032 (1990).
 30. C. Abate, D. Luk, E. Gagne, R. G. Roeder, T. Curran, *Mol. Cell. Biol.* 10, 5532 (1990).
 31. In vitro transcription reactions were carried out in Narnalwa nuclear extracts as described (24). Fos and Jun proteins and truncated NFATp (NFAT-pXS) were used at 500 μ M, and plasmid templates linearized by Eco RI were used at 80 μ g/ml. Transcripts purified from the reactions were analyzed by polyacrylamide gel electrophoresis (PAGE) and quantitated with the use of a phosphorimager.
 32. We thank R. Robinson and M. Gordy for technical assistance and S. Harrison and L. Glimcher for critical reading of the manuscript. Supported by NIH grants CA42471 and GM46227 and a grant from Hoffmann-La Roche, Inc. (to A.R.), NIH grant NS25078 (to P.G.H.), and a grant from the Institute of Chemistry and Medicine funded by Hoffmann-La Roche, Inc. (to G.L.V.). P.G.M. is a Special Fellow of the Leukemia Society of America, J.J. is a Fellow of the Medical Foundation, and T.K.K. is a Fellow of the Helen Hay Whitney Foundation.

28 July 1993; accepted 24 September 1993

Nonuniform Probability of Glutamate Release at a Hippocampal Synapse

Christian Rosenmund,* John D. Clements,† Gary L. Westbrook‡

A change in the probability of neurotransmitter release (P_r) is an important mechanism underlying synaptic plasticity. Although P_r is often assumed to be the same for all terminals at a single synapse, this assumption is difficult to reconcile with the nonuniform size and structure of synaptic terminals in the central nervous system. Release probability was measured at excitatory synapses on cultured hippocampal neurons by analysis of the progressive block of *N*-methyl-D-aspartate receptor-mediated synaptic currents by the irreversible open channel blocker MK-801. Release probability was nonuniform (range of 0.09 to 0.54) for terminals arising from a single axon, the majority of which had a low P_r . However, terminals with high P_r are more likely to be affected by the activity-dependent modulation that occurs in long-term potentiation.

The probability of transmitter release (P_r) from individual synaptic terminals can be estimated from excitatory postsynaptic current (EPSC) amplitude fluctuations by the use of a statistical model of the release process (quantal analysis) (1, 2). This approach is complicated if P_r is not the same for all terminals (2). It is difficult to estimate P_r at central synapses because miniature EPSC amplitudes are close to the intrinsic recording noise level and are high-

ly variable (2, 3). Furthermore, the assumptions underlying statistical models of transmitter release may not always be appropriate at central synapses (2, 4). For instance, the standard binomial model assumes that P_r is uniform at all synaptic terminals. To test directly for nonuniform P_r , we developed an alternative to quantal analysis.

Whole-cell recordings were made from single cultured rat hippocampal neurons that formed recurrent (autaptic) synapses (5). Recordings of *N*-methyl-D-aspartate (NMDA) receptor-mediated EPSCs were made before and during exposure to the NMDA open channel blocker, MK-801 (5 to 20 μ M) (6). Channels were irreversibly blocked under our recording conditions (7). The MK-801 exposure increased the decay rate of the EPSC (Fig. 1, A and B) and, with repeated stimuli, progressively reduced its amplitude (Fig. 1A). The progressive

block rate was measured by the fitting of a single exponential to the EPSC peak amplitude plotted against stimulation number. The rate of progressive block reflects, in part, P_r . If P_r is high then more terminals will release transmitter, more postsynaptic NMDA channels will open, and the progressive block should be more rapid. Consistent with this hypothesis, the progressive block rate was proportional to P_r (Fig. 1, C and D). Raising the calcium concentration increased the EPSC amplitude in the absence of MK-801 (Fig. 1C), and the progressive block rate in MK-801 (5 μ M) increased proportionally (Fig. 1D) (8). Thus, the progressive block rate provides a relative measure of P_r . To obtain a quantitative measure of P_r , estimates of the time course of glutamate in the synaptic cleft, NMDA channel open probability (P_o) and MK-801 binding rate are also required. All these parameters have been measured (6, 9–11), but P_o was obtained from outside-out patch or whole-cell recordings that include extrasynaptic channels (6, 11). Therefore, we examined the P_o of synaptically activated NMDA channels.

Channel open probability has been calculated from the progressive block of NMDA currents by MK-801 (11), but this approach cannot be applied to synaptic currents because progressive block is also influenced by P_r . However, the faster decay rate of NMDA receptor-mediated EPSCs in the presence of MK-801 (Fig. 1B) can be used to estimate P_o . This rate can be used because the irreversible block of open channels early in the synaptic response prevents reopenings later in the response and thus accelerates the EPSC decay (11). This acceleration increases with increasing P_o . A chemical kinetic model (9) (Fig. 2A inset) was used to fit the time course of the synaptic current recorded in the absence and presence of MK-801 (5 μ M) (Fig. 2A) (12). The channel opening rate was the only free parameter in the kinetic model that affected the change in decay rate produced by MK-801, and it had an optimum value of 12.4 ± 0.7 s⁻¹ (mean \pm SEM, $n = 11$). Channel open probability was then calculated from the opening and closing rates (r_o and r_c , respectively) with the equation $P_o = r_o / (r_o + r_c)$; P_o was 0.053 ± 0.003 ($n = 11$). The open probability of an NMDA channel at the peak of a synaptic response (P_o^*) was also calculated from the optimum kinetic model to be 0.041 ± 0.003 ($n = 11$). This probability is less than P_o because some desensitization and agonist dissociation occur during the rising phase of the response. Our estimate of P_o^* was significantly lower than that for channels in outside-out patches ($P_o^* = 0.27$) (11). This discrepancy was not due to differences in the analysis procedures (13). The lower

C. Rosenmund and J. D. Clements, Vollum Institute, Oregon Health Sciences University, Portland, OR 97201.

G. L. Westbrook, Vollum Institute and Department of Neurology, Oregon Health Sciences University, Portland, OR 97201.

*Present address: The Salk Institute, La Jolla, CA 92037.

†Present address: Division of Neuroscience, Australian National University, Canberra, ACT, Australia.

‡To whom correspondence should be addressed.